SERI/TP-254-3799
UC Category: 261
DE90000343

Comparison of Wind Tunnel Airfoil Performance Data with Wind Turbine Blade Data

C. P. Butterfield
G. N. Scott
W. Musial

July 1990

presented at the 25th Intersociety
Energy Conversion Engineering Conference
(sponsored by American Institute of
Aeronautics and Astronautics)
Reno, Nevada
12-17 August 1990

Prepared under Task No. WE011001

Solar Energy Research Institute
A Division of Midwest Research Institute

1617 Cole Boulevard
Golden, Colorado 80401-3393

Prepared for the
U.S. Department of Energy
Contract No. DE-AC02-83CH10093

NOTICE

Printed in the United States of America
Available from:
National Technical Information Service
U.S. Department of Commerce
5285 Port Royal Road
Springfield, VA 22161

Price: Microfiche A01
Printed Copy A02

Codes are used for pricing all publications. The code is determined by the number of pages in the publication. Information pertaining to the pricing codes can be found in the current issue of the following publications which are generally available in most libraries: *Energy Research Abstracts (ERA); Government Reports Announcements* and Index (*GRA* and I); *Scientific and Technical Abstract Reports (STAR)*; and publication NTIS-PR-360 available from NTIS at the above address.

Comparison of Wind Tunnel Airfoil Performance Data with Wind Turbine Blade Data

C. P. Butterfield, George Scott, Walt Musial

Solar Energy Research Institute
1617 Cole Boulevard
Golden, CO 80401 USA

Abstract

Horizontal-axis wind turbine (HAWT) performance is usually predicted by using wind tunnel airfoil performance data in a blade element momentum theory analysis. This analysis assumes that the rotating blade airfoils will perform as they do in the wind tunnel. However, when HAWT performance is measured in full-scale operation, it is common to find that peak power levels are significantly greater than those predicted. This has led to empirical corrections to the predictions. Viterna and Corrigan [10] proposed the most popular version of this correction. But very little insight has been gained into the basic cause of this discrepancy. The Solar Energy Research Institute (SERI), funded by the U.S. Department of Energy (DOE), has conducted the first phase of an experiment focused on understanding the basic fluid mechanics of HAWT aerodynamics. Results to date have shown that unsteady aerodynamics exist during all operating conditions and dynamic stall can exist for high yaw angle operation. Stall hysteresis occurs even for small yaw angles, and delayed stall is a very persistent reality in all operating conditions. Delayed stall is the result of a leading-edge suction peak remaining attached through angles of attack (AOAs) up to 30 deg. Wind tunnel results show this peak separating from the leading edge at 18 deg AOA. The effect of this anomaly is to raise normal force coefficients and tangent force coefficients for high AOA. Increased tangent forces will directly affect HAWT performance in high wind speed operation.

This report describes pressure distribution data resulting from both wind tunnel and HAWT tests. A method of bins is used to average the HAWT data, which are compared to the wind tunnel data. The analysis technique and the test setup for each test are described.

Introduction

Wind turbine operating experience has shown that current analysis techniques are inadequate when used to predict peak power and loads on a fixed-pitch wind turbine. Viterna and Corrigan [10] and Musial and Butterfield [5] both show evidence of high measured power levels due to delayed stall on a 200-kW and a 20-kW HAWT. Because performance and loads are the most important design information needed for successful turbines, it is important to understand the cause of the discrepancy. The primary question is, do the wind tunnel airfoil data accurately represent the airfoil performance on an operating HAWT? SERI has been conducting a comprehensive test program focused on answering this question and understanding the basic fluid mechanics of rotating HAWT stall aerodynamics.

The basic approach used a well-documented airfoil on a HAWT and measured operating pressure distributions at one spanwise location on the blade. Comparisons were then made between the HAWT data and the wind tunnel data. Unfortunately, the early wind tunnel data, available from Somers [8] and Gregorek [3], included AOA ranges only up to 18 deg. This is the angle at which leading-edge stall occurs in the two-dimensional wind tunnel tests. But the major discrepancies occurred near and beyond stall. This meant additional, high-AOA data were needed to study the post-stall behavior. To minimize wind tunnel blockage effects, the 8'-×-12' Colorado State University environmental tunnel was used. The wind tunnel model and test turbine were set up with identical pressure tap locations and pressure measurement equipment. Measurements were taken for a range of Reynolds numbers and AOAs. This report describes the test setup of both the wind tunnel and wind turbine along with results from both.

Wind Tunnel Test Setup

The Colorado State University (CSU) Environmental Wind Tunnel was originally designed for studying wind flow over models of cities and buildings. The test section was reduced to 3.66 m (12 ft) by 1 m (39 in.), which allowed a 1-m airfoil test section to be inserted across the narrow dimension. This resulted in a wide test section, which would minimize the blockage effects. The solid blockage was 0.28% per Thom's method described in Rae and Pope [6]. Figure 1 shows the general layout of the tunnel and the modifications made for this test. The modified open-circuit tunnel was capable of a maximum velocity of 27 m/s (88 ft/s), which resulted in a Reynolds number (RN), based on the 0.46-m (1.5-ft) chord, of 650,000. This value of RN is lower than the HAWT test conditions of 880,000 at the 80% blade span, but it was felt that previous wind tunnel data would accurately describe the airfoil performance for values of RN from 750,000 to 3 million for values of AOA less than 20 deg.

Pressure distribution measurements were made on the model along with pitot tube measurements two chord lengths displaced from each side of the model and one chord length upwind of the model leading edge. Tunnel temperature, probe total pressure, local flow angle at 0.6 chord ahead of the leading edge, and model pitch angle relative to the tunnel axis were also measured.

Usually, airfoil drag is determined by measuring the velocity profile in the wake of the airfoil and then equating the momentum deficit in that wake to the total drag. This requires a movable pitot tube or a wake rake positioned downwind of the airfoil. It was not possible to make these measurements on the rotating wind turbine blade. There is also evidence that this technique is inaccurate when large-scale separation caused by rotational flow in the wake is present. Because SERI's focus was on stall behavior, in which large-scale separation is always present, it was decided that only pressure drag (C_{Dp}) would be measured. Because C_{Dp} is determined from pressure distribution integrations, as described by Rae and Pope [6], wind tunnel data could be compared with HAWT data directly.

Tunnel turbulence level was a major concern. High-frequency turbulence can affect the airfoil boundary layer and thus the performance. To address this concern, a pitot-tube traverse test and a hot-wire traverse test were conducted. The traverses were performed across the test section midspan in the same location as the model. The results of the first test, shown in Figure 2, describe a 6-cm (2.5-in.) boundary layer at the tunnel wall and an acceptable flat velocity distribution across the tunnel. The results of the second, hot-wire traverse confirmed the location of the boundary layer. A value of 1% turbulence intensity was measured at the midspan of the test section. This is a high value for airfoil

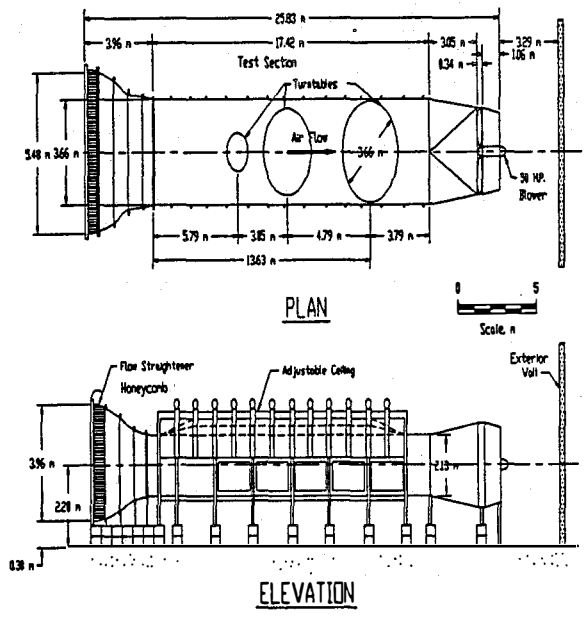

Figure 1. Wind tunnel layout, Colorado State University

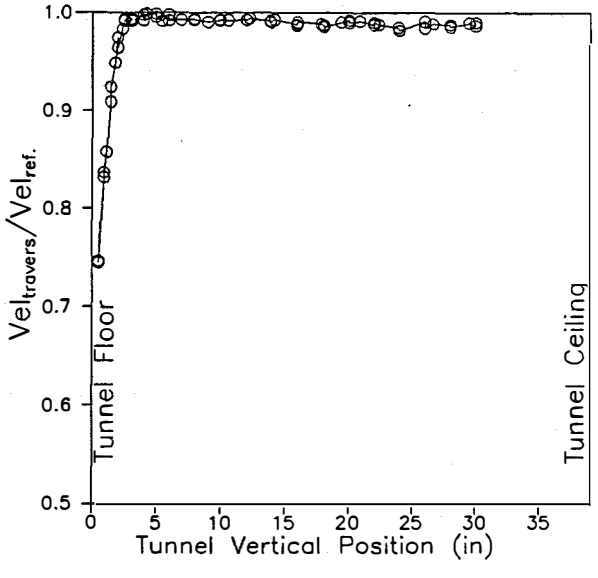

Figure 2. Wind tunnel velocity profile

testing, but the important consideration is the scale of the turbulence. If the scale is close to that of the airfoil boundary layer, it can trip laminar flow into turbulent flow and thus modify performance. If the scale is large, there should be little effect. Figure 3 shows a plot of the power spectral density (PSD) of the hot-wire data at the tunnel midspan at a tunnel speed of 24.5 m/s (80 ft/s). The PSD has been multiplied by frequency and normalized by the standard deviation squared. The area under the curve is unity and represents the measured turbulent intensity of 1%. It is clear that the majority of the energy is below 1 Hz (24-m scale). This scale of turbulence is much larger than the boundary layer and therefore should have minimal effect on the performance of the airfoil. These fluctuations were caused by small changes in average tunnel speed control.

The airfoil model was 99 cm (39 in.) long with a chord of 45.7 cm (18 in.). It was placed in the wind tunnel, bridging the narrow dimension (99 cm). This allowed the wake of the airfoil to expand across the 3.67-m dimension of the tunnel. A rubber seal was placed between the wall of the tunnel and the end of the model to prevent leaks. The model was fabricated from the blade molds used to build the blades. This was done to ensure that the model would accurately represent the HAWT blade. Pressure taps were installed inside the model using stainless steel tubing 25-38 cm long of 1-mm inside diameter. Each tube led from the airfoil surface to a pressure transducer mounted inside the model. The 31 pressure tap locations and installations were identical to the HAWT blade installation.

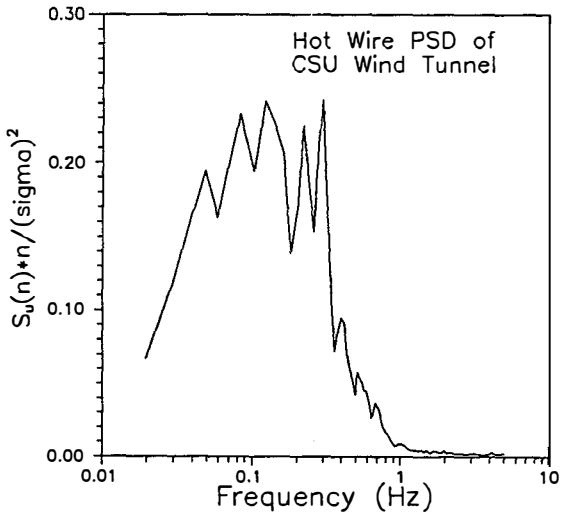

Figure 3. Power spectral density of hot-wire data at tunnel test section midspan

The model also included a local flow angle (LFA) probe and a total pressure probe mounted on the leading edge. A lightweight fiberglass flag 5 cm (2 in.) long was used to sense local flow angles. The same probe was mounted on the HAWT blade. To accurately account for the induced upwash effect on this LFA probe, measurements were taken during the wind tunnel tests and compared with previous measurements made at RN = 1 million. Butterfield [1] describes the LFA probe and previous calibration measurements of this probe in the Ohio State University wind tunnel. Each data channel was filtered with a roll-off frequency of 100 Hz and then sampled at 520 Hz using a pulse-code-modulation (PCM) encoder. The PCM stream was recorded on a Honeywell 101 tape recorder and later decoded and analyzed. Butterfield et al. [2] and Simms and Butterfield [7] describe the pressure system instrumentation and recording equipment in detail.

Wind Turbine Test Setup

The turbine used was a 10-m-diameter, three-bladed, downwind machine mounted on a guyed tower. The blades were variable pitch, constant chord, with zero twist. The S809 airfoil used throughout the blade was a laminar flow design with 21% thickness. This airfoil was designed specifically for wind turbine applications. Tangler [9] describes the airfoil and design objectives. Figure 4 describes the test turbine. This figure also shows a video camera mounted on

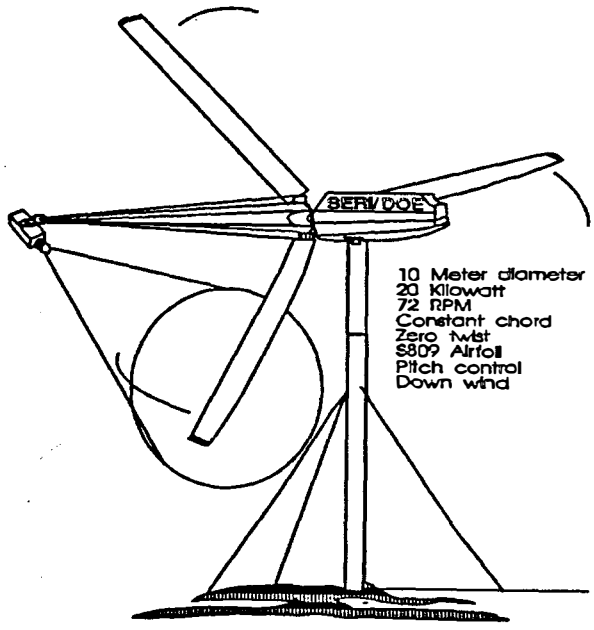

Figure 4. Test turbine description

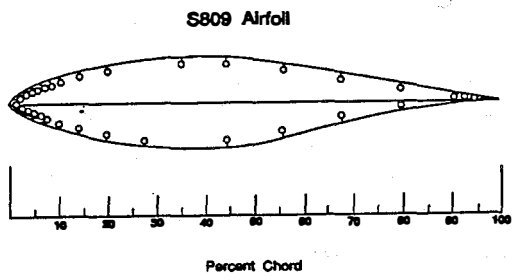

Figure 5. Airfoil and pressure tap description

a boom that extends downwind of the rotor. The video camera was used to view flow patterns represented by tufts attached to the low-pressure side of the blade.

The pressure taps were located along a chordwise line at the 80% blade span. Figure 5 shows the airfoil and the pressure tap locations. Close spacing of the taps near the leading-edge provided reasonable resolution of the leading-edge suction peak. The tube lengths were identical to those in the wind tunnel model resulting in measured acoustic fundamental frequencies from 85 to 95 Hz. Close examination of PSD functions of the integrated pressure distributions revealed no significant energy for frequencies greater than 20 Hz. Because the frequency response function is nearly flat in this region, no corrections were necessary.

Data Analysis

The wind tunnel data were steady and therefore needed no special processing. Pressure measurements were normalized by local tunnel dynamic pressure to get pressure coefficients (C_p). Pressure coefficient distributions were integrated around the airfoil to obtain values of normal force coefficient (C_n), tangent force coefficient (C_T), and pitching moment coefficient (C_m). These were used along with AOA measurements to calculate lift and pressure drag coefficients (C_L, C_{Dp}), using the method described by Rae and Pope [6].

The HAWT data were unsteady, requiring special data processing to obtain averaged values of C_n, C_T, and pressure distributions. The data were averaged by a technique known as the method of bins. This technique assigns each data sample to one of a set of "bins" based on the value of the independent variable—in this case, the angle of attack. The bins in this study were 1 deg wide, and started at 0 deg.

In this technique each sample is read and its bin number determined from its angle-of-attack value. The corresponding bin counter is incremented, and the current pressure values are added to the cumulative totals for each pressure tap. When all the data have been read, the pressure totals are divided by the number of samples in the bin, giving an average pressure distribution for the bin. Other statistics, such as standard deviation, skew, and kurtosis, are also computed.

The original analog signals from the HAWT tests were passed through a four-pole Butterworth filter with a roll-off point at 100 Hz and then digitized at a 522-Hz sample rate. The resulting data stream was block-averaged to a final output rate of 10 Hz. These low-rate data were used as the input to the binning process.

Wind Tunnel Results

A comparison of C_L data recorded from the three different wind tunnels was made first to establish a baseline validity check on the CSU wind tunnel data. As can be seen in Figure 6, the curves do not all look exactly alike. The Reynolds numbers for all three are not the same, which could be one of the explanations. But in general, the comparison is reasonable. The slope of each curve is approximately the same, the zero lift angle is similar, and $C_{L(max)}$ is similar but decreases with RN. Figure 7 shows how $C_{L(max)}$ decreases with RN and compares the general trend with the NACA 4412 and NACA 64-418 airfoils. This comparison shows that it is reasonable to expect a drop in $C_{L(max)}$ in the CSU data due to RN. Additional data will be presented in the following HAWT comparisons section.

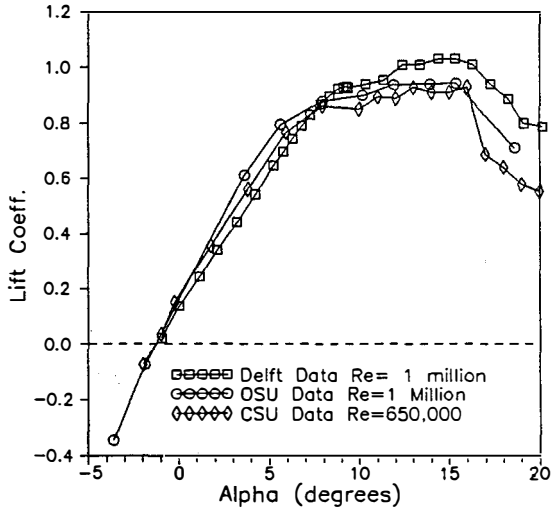

Figure 6. Wind tunnel C_l comparisons

From these comparisons, it seemed that the CSU data did not match previous wind tunnel data perfectly, but they were the best to use in HAWT comparisons because they represented the performance of an exact copy of the airfoil and instrumentation of the HAWT blade. Any differences between this set of data and the HAWT data would most likely be explained by real differences occurring between two-dimensional wind tunnel conditions and three-dimensional wind turbine aerodynamics. The CSU data also contained values of AOA up to 90 deg. Previous wind tunnel test data only had values up to 20 deg. High values of AOA were needed to compare deep-stall HAWT data to wind tunnel data. Figure 8 shows the results of the high-AOA data for a tunnel speed of 26 m/s (88 ft/s) and Reynolds number equal to 650,000.

Comparison with HAWT Data

Figure 9 shows lift coefficient data for both the HAWT and CSU wind tunnel. The AOA used for the HAWT data is measured LFA data corrected for upwash effects using corrections derived from the wind tunnel tests. Wind tunnel AOA values are the usual direct, chord line angle measurements. The wind tunnel data are steady; the HAWT data are very unsteady and must be averaged in the manner described earlier. Plotted along with the HAWT data are the ±1 standard deviation lines. This comparison shows that the wind turbine airfoil does not experience a sudden drop in C_L at stall as it does in the wind tunnel. Increased standard deviations near and beyond stall highlight the unsteady nature of the stall process.

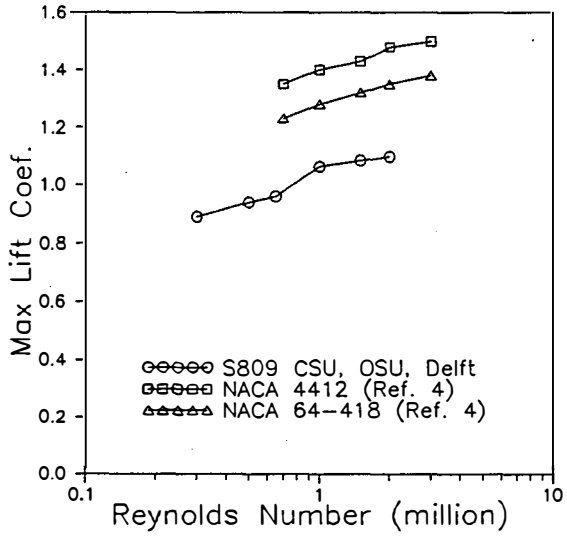

Figure 7. Reynolds number effects on $C_{l_{max}}$

Figure 10 compares C_T data from the wind tunnel and HAWT. Again, the wind tunnel data experience a dramatic drop at stall while the C_T on the HAWT airfoil drops far more gradually. In this case, the difference between the two data sets beyond stall is dramatic, especially considering the fact that C_T is the primary force causing torque and power on a wind turbine. This difference could cause significant errors in predicted turbine performance.

Pressure distributions were compared for a variety of AOAs. For low AOA, the differences were insignificant. Figure 11 shows pressure distributions

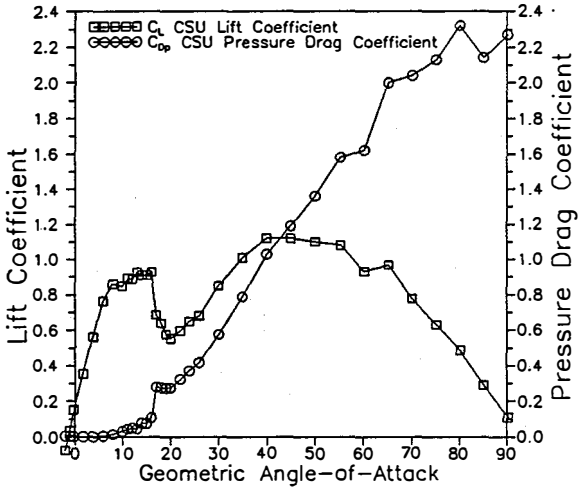

Figure 8. High-AOA airfoil performance results

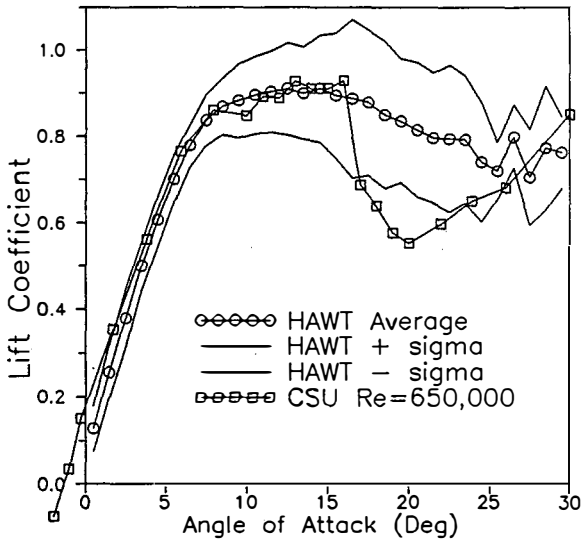

Figure 9. Wind tunnel HAWT comparison

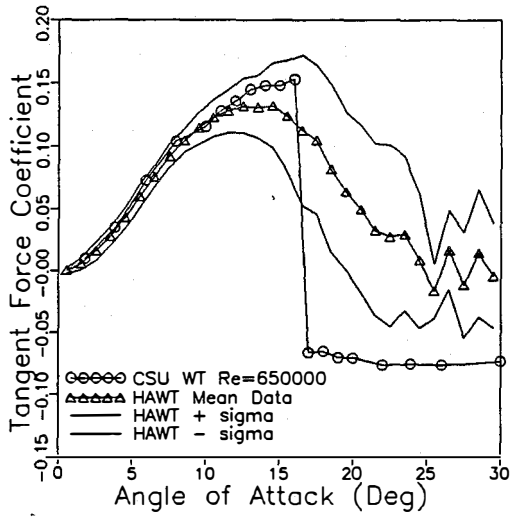

Figure 10. Wind tunnel HAWT comparison for tangent coefficient

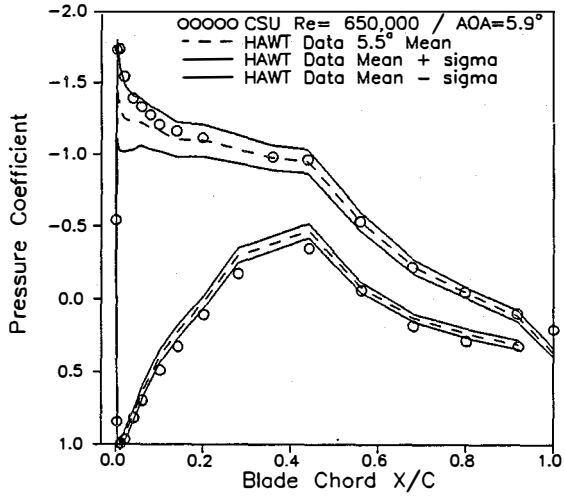

Figure 11. Pressure distribution comparison for AOA = 5°

for 5 deg AOA (5 deg < AOA < 6 deg) from the wind tunnel and the bin-averaged HAWT data. The differences are within the standard deviation of the HAWT data. Figure 12 shows the same comparison for 16 deg (16 deg < AOA < 17 deg). The low-pressure side of the airfoil shows the separation point (where the distribution goes flat) at 35% chord for the wind tunnel data. However, the HAWT data show this separation point at 55% chord. There also appear to be some differences in the magnitudes of the pressure coefficients on the high-pressure side of the airfoil (bottom part of the curve), but the general shape is similar, implying that no large differences exist in flow separation or velocity distribution.

Figure 13 shows data from the 18-deg bin. The suction peak is lost because of leading-edge separation for the wind tunnel data. However, the HAWT data indicate that the flow is still attached because the suction peak still exists. Figure 14 indicates that this persistent suction peak exists at angles up to a 30-deg AOA. The reason for this behavior is not known. But it has been speculated that spanwise flow in the separated flow region is creating a favorable pressure gradient near the boundary layer separation interface. Studies are being conducted to investigate this possibility.

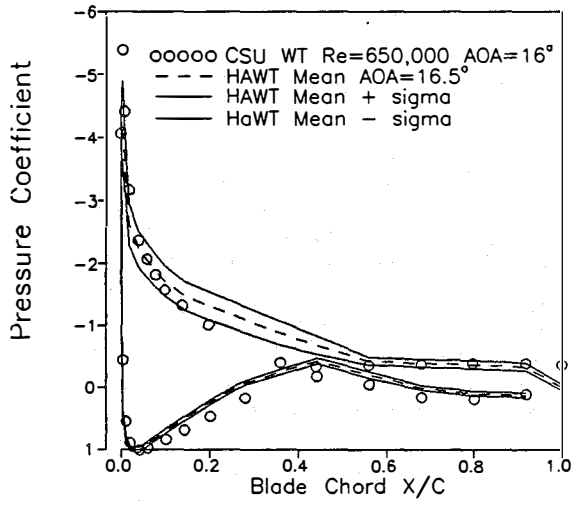

Figure 12. Pressure distribution comparison for AOA = 16°

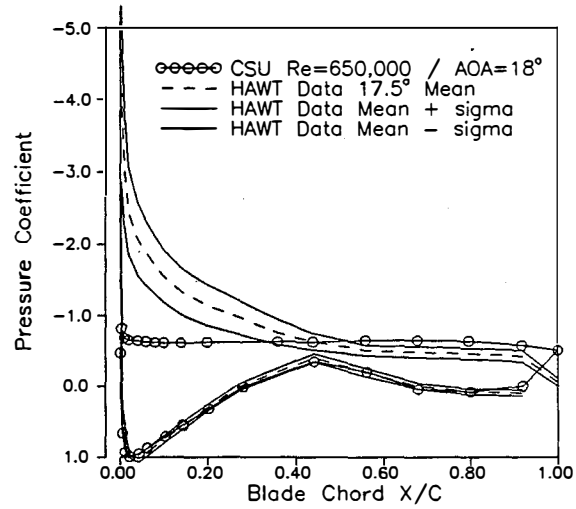

Figure 13. Pressure distribution comparison for AOA = 18°

Standard deviations in the pressure distributions near the suction peak become large during deep stall. There was some speculation that this resulted from two distinct flow states, one with no leading-edge suction peak and the other with a strong suction peak. The mean of these two states might be represented by the dashed line curve in Figure 13. This might occur if dynamic stall were dominating the airfoil performance.

To investigate this possibility, a distribution of samples was plotted for a pressure tap in the suction peak. If this distribution were bimodal, it would indicate that two different flow conditions did exist. However, if the distribution were unimodal, then the high standard deviation would indicate unsteadiness or randomly distributed samples. In the latter case, the average values would be an accurate representation of the pressure distributions that designers should use in their analyses. Figure 15 shows the sample probability density compared to a Gaussian (normal) distribution for the 7.9% chord pressure tap located on the suction side of the airfoil. These data represent the AOA range from 18 to 20 deg. The sample distribution appears to be Gaussian. It was concluded that the mean values did indeed represent a unique flow state, one that was very different from the flow state for the same airfoil in the wind tunnel.

Conclusions and Future Work

The averaged data presented indicate that the S809 airfoil stalls far more gently on a wind turbine than it does when tested in a wind tunnel. The difference is because persistent suction peaks remain attached at the leading edge beyond normal wind tunnel stall AOA. For AOAs below stall, the average airfoil behavior appears to be similar to the wind tunnel performance. Wind turbine designers should be aware of these differences when designing stall control wind turbine blades or they may underestimate the peak performance and loads. It is not clear what the dynamic effects were on these results. The flow conditions were unsteady and should be analyzed again using data analysis techniques that isolate the unsteady effects. It is also important to examine spanwise effects on these results. Future work will focus on these issues as well as the effect of turbulence on airloads and structural loads.

Acknowledgments

This work was sponsored by the U.S. DOE under contract number DE-AC02-83CH10093. The authors would like to thank Dave Simms and Mike Jenks for all the work they contributed to this project and Bob Thresher for his constant support and guidance.

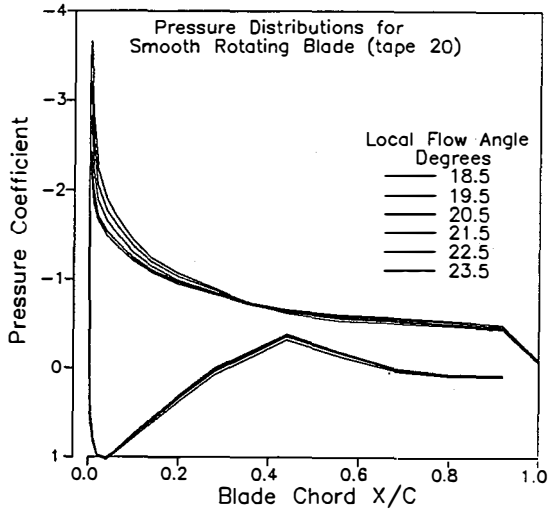

Figure 14. Bin-averaged pressure distributions for high AOA

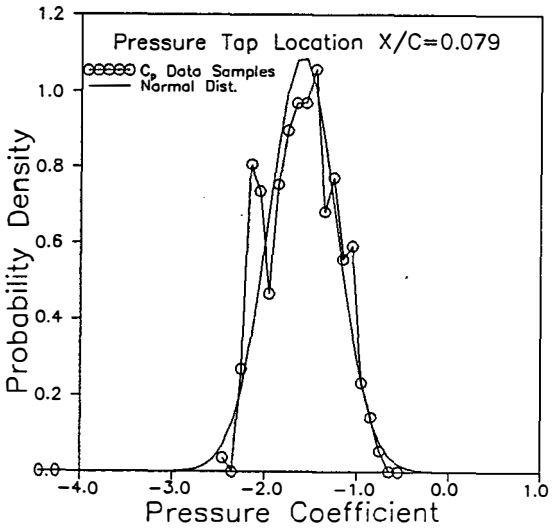

Figure 15. Sample distribution of C_p data for suction peak tap

References

Butterfield, C. P., June 1989, *Three-Dimensional Airfoil Performance Measurements on a Rotating Wing*. SERI/TP-217-3805, Golden, CO: Solar Energy Research Institute. Prepared for the European Wind Energy Conference and Exposition, Glasgow, Scotland, 10-13 July, 1989.

Butterfield, C. P., M. D. Jenks, D. A. Simms, and W. P. Musial, *Aerodynamic Pressure Measurements on a Rotating Wind Turbine Blade.* SERI/TP-257-3695, Golden, CO: Solar Energy Research Institute.

Gregorek, G. M., unpublished report of Ohio State University testing of S809 in November 1989.

Hoerner, S. F., 1975, *Fluid-Dynamic Lift.* Los Angeles, CA: Hoerner.

Musial, W. D., C. P. Butterfield, and M. D. Jenks, February 1990, *Comparison of Two- and Three-Dimensional S809 Airfoil Properties for Rough and Smooth HAWT Rotor Operation.* SERI/TP-257-3603, Golden, CO: Solar Energy Research Institute. Prepared for the 9th ASME Wind Energy Symposium, 14-18 January 1990, New Orleans, Louisiana.

Rae, H. W., and A. Pope, 1984, *Low-Speed Wind Tunnel Testing.* New York: John Wiley & Sons.

Simms, D. A., and C. P. Butterfield, February 1990, *PC-Based PCM Telemetry Data Reduction System Hardware.* SERI/TP-257-3662, Golden, CO: Solar Energy Research Institute. Prepared for the 36th ISA International Instrumentation Symposium, Denver, Colorado, 7-10 May 1990.

Somers, D. M., March 1989, *Design and Experimental Results for the S809 Airfoil.* Golden, CO: Solar Energy Research Institute (unpublished contractor report).

Tangler, J. L., December 1987, *Status of the Special-Purpose Airfoil Families.* SERI/TP-217-3264, Golden, CO: Solar Energy Research Institute. Prepared for Windpower '87, San Francisco, California, 5-8 October 1987.

Viterna, L. A., and R. D. Corrigan, 1981, *Fixed Pitch Rotor Performance of Large Horizontal-Axis Wind Turbines.* DOE/NASA Workshop on Large Horizontal-Axis Wind Turbines, Cleveland, Ohio, July 28-30.